2021 43rd Annual International Conference of the
IEEE Engineering in Medicine & Biology Society (EMBC)
Oct 31 - Nov 4, 2021. Virtual Conference

Using physiological parameters measured by hyperspectral imaging to detect colorectal cancer

Marianne Maktabi[1], Mariia Tkachenko[1], Hannes Köhler[1], Katrin Schierle[3], Ines Gockel[2], Boris Jansen-Winkeln[2], Claire Chalopin[1]

Abstract— **The accurate detection of malignant tissue during colorectal surgery impacts operation outcome. The non-invasive spectral imaging combined with machine learning (ML) methods showed to be promising for tumor identification. However, large spectral range implies large computing time. To reduce the number of features, ML methods (e.g. logistic regression and convolutional neuronal network CNN) were evaluated based on four physiological tissue parameters to automatically classify cancer and healthy mucosa in resected colon tissue. A ROC AUC of 0.81 was achieved with the CNN. This study shows that the use of only specific wavelengths bands can detect cancer.**

Clinical Relevance— **These outcomes support the possibility to automatically classify colon tumor based on physiological parameters calculated using only specific wavelength bands. Hence, future image-guided colorectal surgeries can be performed with real-time multispectral imaging.**

I. Introduction

Colorectal cancer is the fourth deadliest cancer in the world [1]. Early diagnosis by biopsy is important to reduce mortality. Furthermore, the quality of the surgical intervention, which represents the reference therapy for advanced cancers, is also crucial to achieve curative treatment. The operation outcomes depend on the complete removal of the tumor. Therefore, the detection of the tumor borders is extremely important. Currently, the surgeon inspects the resected tissue visually and tactilely.

New imaging technologies offer possibilities to support the surgeon during operations and biopsies. Medical hyperspectral imaging (HSI) is a non-invasive and contactless technology that provides information about tissue properties [2]. The principle is the measurement of light interaction with tissue (reflectance, absorption, scattering) using optical sensors and a camera. In addition, physiological parameters such as tissue oxygenation saturation can be determined based on specific spectral bands in the visual and near-infrared electromagnetic wavelength range [3]. A great advantage of this imaging method is that it can be easily integrated with surgical laparoscopes or endoscopes [4].

Several studies have already shown that colorectal cancer can be successfully recognized using reflection spectra. Classification of colorectal cancer on specimens was done using simple threshold value using linear discriminant analysis (LDA) [5], neural networks [6], and convolutional neural networks (CNN), such as hybrid CNN as a combination of 2D- and 3D-CNN and the ResnetCNN [7]. One limitation of these powerful methods is the large computing time when large spectral range is used. This is not compatible with intraoperative use.

Therefore, we present in this paper a classification approach based on four different physiological parameters. These are computed using known restricted wavelength bands. We described in a previous paper that physiological parameters show different values between healthy tissue and tumors, different tumor grades, and tumors treated with different therapies [6]. Based on these findings, this work aims to investigate whether it is possible to successfully identify cancerous tissue based on physiological parameters. For this purpose, classical machine learning (ML) methods and deep convolutional neural networks (CNN) were implemented and evaluated in a leave-one-patient-out cross-validation (LOPOCV) and a 5-fold cross-validation (5-fold CV).

II. Methods

Fig. 1 shows the processing steps of the approach, which are presented in this section.

A. Patient data

The study was performed at the University Hospital of Leipzig, Germany, which was approved by the local ethics committee of the Leipzig University (026/18-ek) and registered at Clinicaltrials.gov (NCT04230603). It was conducted during July 2019 and May 2020 and includes 52 patients who underwent a colorectal surgery. 18 of them received neodjuvant treatment and 25 patients had malignant tumors of different TNM types.

[1] Marianne Maktabi, Hannes Köhler, Claire Chalopin are with Innovation Center Computer-Assisted Surgery (ICCAS), Leipzig University, Post code Leipzig, Germany; marianne.maktabi@medizin.uni-leipzig.de (M.M.)

[2]Ines Gockel, Boris Jansen-Winkeln are with Department of Visceral, Transplant, Thoracic and Vascular Surgery, University Hospital of Leipzig, Post code Germany

[3]Katrin Schierle Institute of Pathology, University Hospital Leipzig, Post code Leipzig, Germany; Katrin.Schierle@medizin.uni-leipzig.de

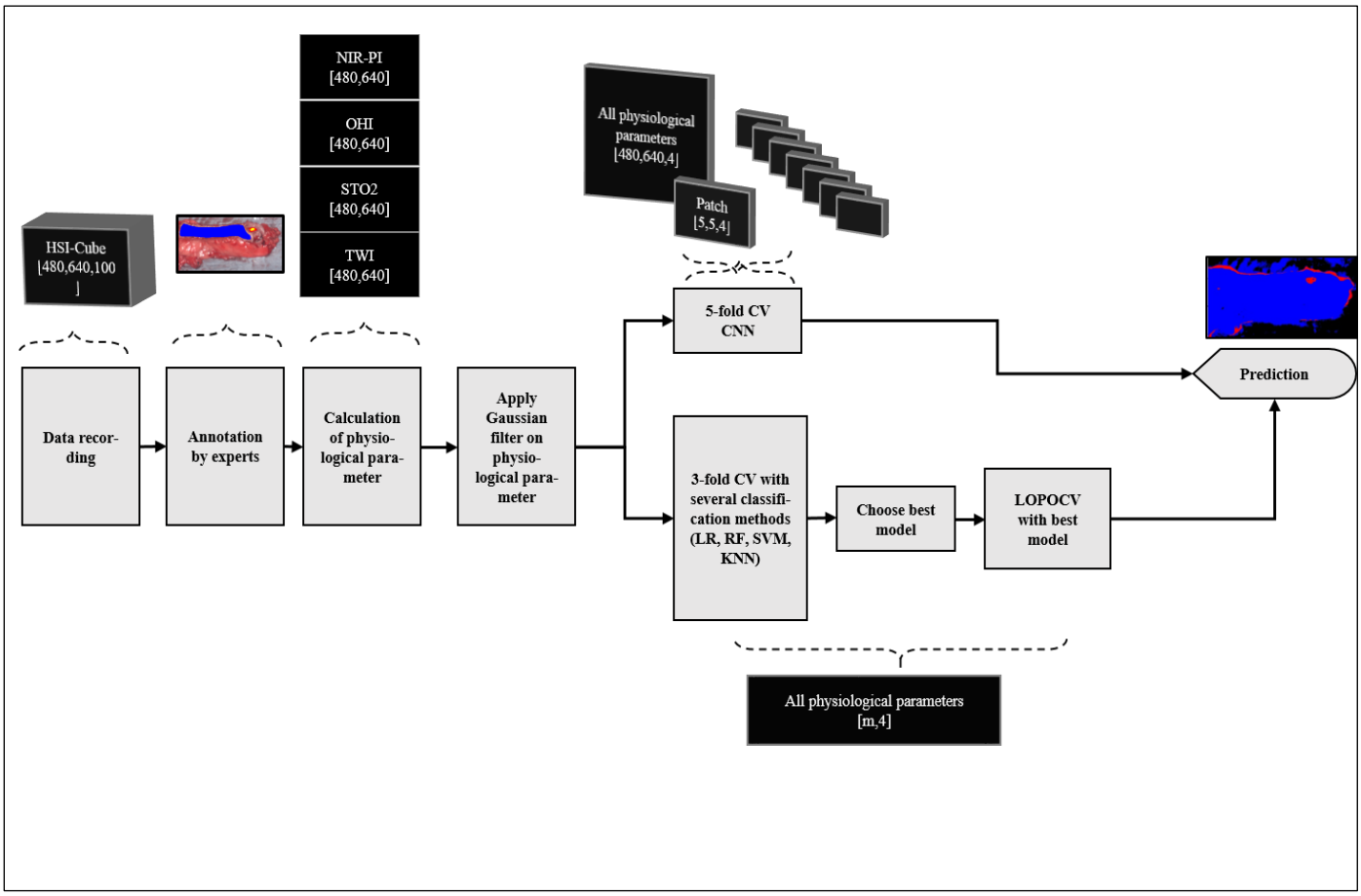

Figure 1 Pipeline of the working process.

B. Surgical procedure and image recording

Resected colon tissue was lengthwise cut through and the inside tissue imaged using the HSI system TIVITA® Tissue system (Diaspective Vision GmbH, Am Salzhaff-Pepelow, Germany). The measurements were done in the operating room within 10 minutes after tissue resection as described in [8]. The acquisition time and spectral range of the HSI data is 6s and 500 to 1000 nm, respectively. Further technical details can be found in [9]. An experienced pathologist and a surgeon annotated the tissue as described in [6]. In this work, two tissue classes are considered: cancer and healthy tissue.

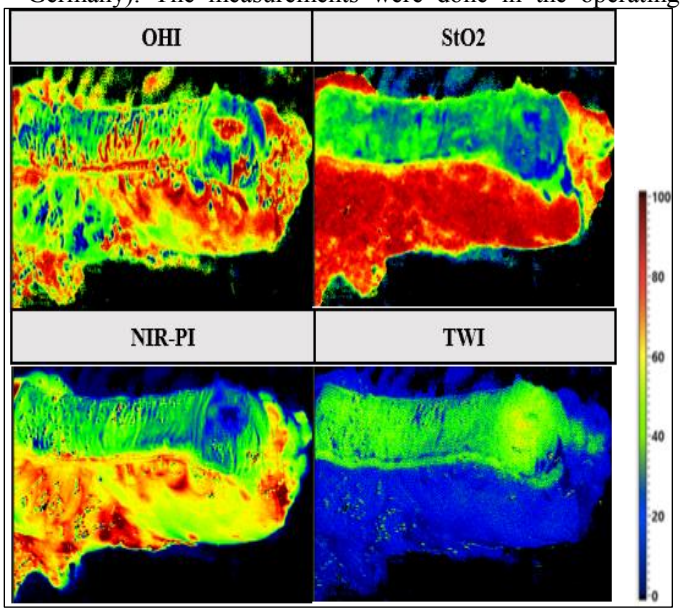

Figure 2 Physiological parameter calculated by using the spectral data.

C. Calculation of the physiological parameters and image preprocessing

Based on the recorded HSI cubes four physiological parameters were calculated according to the algorithms described in [3]:

- tissue oxygenation (StO2),
- near-infrared perfusion index (NIR PI),
- tissue water index (TWI), and
- organ hemoglobin index (OHI) (figure 2).

The StO2 was calculated using the spectral ranges from 570 to 590 nm and 740 to 780 nm. The wavelength ranges from 655-735 nm and 825-925 nm were used to calculate the NIR PI. Hemoglobin is known to absorb light mostly in the ranges 530 to 590 nm and 785 to 825 nm. These were used to calculate the OHI. At 960 nm the water presents a peak in the absorbance spectra. So the TWI was calculated based on spectra values in the range of 880-900 nm and 955-980 nm.

TABLE I. RESULTS: PERFORMANCE OF TWO CLASSIFICATION MODELS IN TERMS OF F1-SCORE, SENSITIVITY, SPECIFICITY AND AUC-SCORE.

	F1 Score		Sensitivity		Specificity		AUC	
	Mean	Std	**Mean**	Std	**Mean**	Std	Mean	Std
Logistic regression	**0.35**	0.26	**0.60**	0.37	**0.73**	0.24	**0.72**	0.25
3D-CNN with inception block	**0.56**	0.28	**0.72**	0.26	**0.90**	0.14	**0.80**	0.17
3D-CNN (11 layers)	**0.51**	0.29	**0.67**	0.29	**0.90**	0.13	**0.78**	0.17

D. Automatic classification

ML methods and, more recently, deep learning approaches were evaluated with HSI data and showed promising results for medical applications [10], [11], [12]. We tested several standard ML and CNN algorithms to detect cancer tissue based on the pixel-wise calculated prediction score. Logistic regression (LR), support vector machine (SVM) with linear and radial basis kernel of degree 3, random forest (RF) with

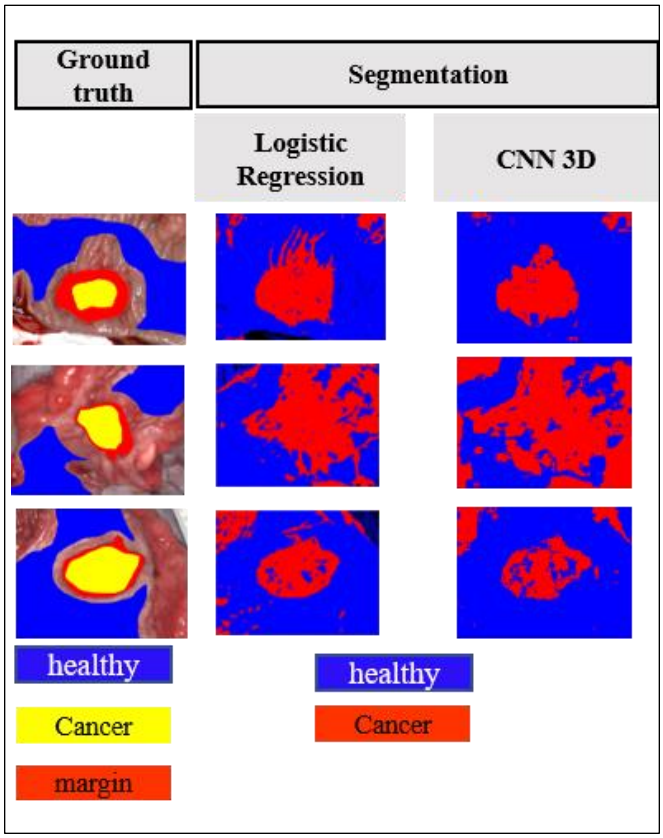

Figure 3 Results for three patients classified by Logistic regression and a 3 dimensional CNN.

100 trees, and k-nearest neighbors (KNN) with 5 neighbors were implemented using Python's Scikit-learn library [13]. Two CNN with 11 Layers and an inception block with 3 layers were implemented using the Tensorflow 2.4., CUDA, and the Adam optimization (0.001). The parameter images were smoothed using a Gaussian filter (kernel size: 21, sigma value: 2) to reduce the image noise previously to the classification step.

E. Implementation and Training

The dataset including the 52 patients is composed of 5,385,018 spectra representing healthy tissue and 495,553 spectra corresponding to cancer. For the standard ML algorithms, the data were balanced by randomly selecting the same number of spectra of healthy tissue and cancer. For the CNNs, we used class weights. These were calculated by dividing the total number of samples by the number of samples per class. The input dataset for the CNN was spatial patches of 5x5 pixels.

Standard ML algorithms were trained and evaluated based on a 3-fold cross-validation on a small dataset (10% of the whole dataset). The best model was evaluated using a LOPOCV. The CNNs were tested by leaving 20% of the patients out. The testing group in each fold was fully independent. The training and validation were performed on patients in the remaining 4 folds. Feature importance was calculated based on the whole dataset using scikit-learn version 0.24.2[14].

F. Performance metrics and statistical methods

Standard metrics, including the Area Under Receiver Operator Curve (ROC-AUC), sensitivity, specificity, and F1-score, were implemented using Python scikit-learn (version 0.23, https://scikit-learn.org) to evaluate the performance of the classifiers. The ROC-AUC can measure the performance of models in unbalanced datasets very well. A two-tailed paired t-test with alpha=0.05 as a significant value was done for statistical analysis using Excel (Microsoft Office 365, Microsoft, U.S.A.).

III. RESULTS

Among the ML algorithms, the SVM with linear kernel and the LR achieved the highest performances with an averaged sensitivity of 0.68 and specificity of 0.75 and 0.74, respectively, in the 3-fold CV. The KNN, MLP, RF, and SVM with radial basis kernel achieved an averaged sensitivity of 0.73, 0.71, 0.78, 0.70, respectively, and an averaged specificity of 0.55, 0.66, 0.53, and 0.73, respectively. Finally, the LR was chosen for the LOPOCV due to its faster model training. On the other hand, the CNN models were trained and evaluated with the complete dataset. The best performance

was achieved by the CNN with inception block with an AUC score of 0.80 Significant performance differences between the LR and CNN models were observed for all performance measurements.

The feature weights' calculation performed on the physiological parameters showed that the NIR PI is the most important parameter, followed by the TWI, StO2, and OHI parameters.

The outcomes of the classification are visualized in Figure 3.

IV. Discusssion

In this work, we evaluated the prediction of cancer based on physiological parameters for the first time using the HSI data of 52 patients who underwent colorectal surgery. We compared several classification models. The CNN showed the highest performance with an AUC score of 0.81. Such comparison results were also obtained in [15] for the discrimination of different healthy tissues (nerve, blood vessels, muscle, fat, skin) based on HSI data. We showed that a simple 3D-CNN trained with only 35,281 features can provide high performance.

In several works, HSI was used to classify colon cancer [5]–[7], [16]. Baltussen et al. achieved the same AUC score of 0.81 using a larger spectral range (400-1700nm) covered by the HS system. We obtained in a previous work a higher AUC score of 97 for cancer detection on the same patient dataset but using all spectral bands (500-1000nm) [6]. In this work, physiological parameters were used as features whose computation require fewer wavelengths. As it was investigated in [6], physiological parameters reflect clear differences between tumor types but also tumor medical pretreatments. To capture these differences, more complex classifier models and larger datasets are necessary.

An interesting further medical application of HSI is its combination with optical gastrointestinal endoscopy for colon cancer diagnosis. New real-time flexible endoscopic HSI systems are described in [17]–[19]. Real-time HSI is achieved with the selection of a limited number of specific spectral bands [7], [20]. Our approach for the prediction of malignant tissue is based on physiological parameters that are calculated using limited areas of the light spectrum. This tool is compatible with real-time endoscopic imaging systems.

Acknowledgment

This study was funded by the Federal Ministry of Education and Research 13GW0248B.

References

[1] E. Dekker, P. J. Tanis, J. L. A. Vleugels, P. M. Kasi, and M. B. Wallace, "Colorectal cancer," *The Lancet*, vol. 394, no. 10207, pp. 1467–1480, Oct. 2019, doi: 10.1016/S0140-6736(19)32319-0.

[2] B. Fei, "Hyperspectral imaging in medical applications," in *Data Handling in Science and Technology*, vol. 32, Elsevier, 2020, pp. 523–565.

[3] A. Holmer, J. Marotz, P. Wahl, M. Dau, and P. W. Kämmerer, "Hyperspectral imaging in perfusion and wound diagnostics – methods and algorithms for the determination of tissue parameters," *Biomedical Engineering / Biomedizinische Technik*, vol. 63, no. 5, pp. 547–556, Oct. 2018, doi: 10.1515/bmt-2017-0155.

[4] H. Köhler *et al.*, "Laparoscopic system for simultaneous high-resolution video and rapid hyperspectral imaging in the visible and near-infrared spectral range," *J. Biomed. Opt.*, vol. 25, no. 08, Aug. 2020, doi: 10.1117/1.JBO.25.8.086004.

[5] R. J. Beaulieu, S. D. Goldstein, J. Singh, B. Safar, A. Banerjee, and N. Ahuja, "Automated diagnosis of colon cancer using hyperspectral sensing," *The International Journal of Medical Robotics and Computer Assisted Surgery*, vol. 14, no. 3, p. e1897, Jun. 2018, doi: 10.1002/rcs.1897.

[6] B. Jansen-Winkeln *et al.*, "Feedforward Artificial Neural Network-Based Colorectal Cancer Detection Using Hyperspectral Imaging: A Step towards Automatic Optical Biopsy," *Cancers*, vol. 13, no. 5, p. 967, Feb. 2021, doi: 10.3390/cancers13050967.

[7] F. Manni, R. Fonolla, S. B. de Koning, and T. Ruers, "Hyperspectral imaging for colon cancer classification in surgical specimens: towards optical biopsy during image-guided surgery," in *2020 42nd Annual International Conference of the IEEE Engineering in Medicine & Biology Society (EMBC)*, Montreal, Canada, Aug. 2020, p. 5, doi: 10.1109/EMBC44109.2020.9176543978-1-7281-1990-8/20/$31.00.

[8] B. Jansen-Winkeln *et al.*, "Determination of the transection margin during colorectal resection with hyperspectral imaging (HSI)," *Int J Colorectal Dis*, vol. 34, no. 4, pp. 731–739, Apr. 2019, doi: 10.1007/s00384-019-03250-0.

[9] A. Holmer, F. Tetschke, H. Malberg, W. Markgraf, C. Thiele, and A. Kulcke, "Oxygenation and perfusion monitoring with a hyperspectral camera system for chemical based tissue analysis of skin and organs," *Physiol. Meas.*, p. 15, 2016.

[10] P. Ghamisi, J. Plaza, Y. Chen, J. Li, and A. J. Plaza, "Advanced Spectral Classifiers for Hyperspectral Images: A review," *IEEE Geoscience and Remote Sensing Magazine*, vol. 5, no. 1, pp. 8–32, Mar. 2017, doi: 10.1109/MGRS.2016.2616418.

[11] S. Ortega, H. Fabelo, D. Iakovidis, A. Koulaouzidis, and G. Callico, "Use of Hyperspectral/Multispectral Imaging in Gastroenterology. Shedding Some–Different–Light into the Dark," *Journal of Clinical Medicine*, vol. 8, no. 1, p. 36, Jan. 2019, doi: 10.3390/jcm8010036.

[12] A. Signoroni, M. Savardi, A. Baronio, and S. Benini, "Deep Learning Meets Hyperspectral Image Analysis: A Multidisciplinary Review," *J. Imaging*, vol. 5, no. 5, p. 52, May 2019, doi: 10.3390/jimaging5050052.

[13] F. Pedregosa *et al.*, "Scikit-learn: Machine Learning in Python," *J. Mach. Learn. Res.*, vol. 12, pp. 2825–2830, Nov. 2011.

[14] L. Breiman, "[No title found]," *Machine Learning*, vol. 45, no. 1, pp. 5–32, 2001, doi: 10.1023/A:1010933404324.

[15] M. Barberio *et al.*, "Deep Learning Analysis of in Vivo Hyperspectral Images for Automated Intraoperative Nerves Detection," In Review, preprint, Apr. 2021. doi: 10.21203/rs.3.rs-393233/v1.

[16] E. J. M. Baltussen *et al.*, "Hyperspectral imaging for tissue classification, a way toward smart laparoscopic colorectal surgery," *Journal of Biomedical Optics*, vol. 24, no. 01, p. 1, Jan. 2019, doi: 10.1117/1.JBO.24.1.016002.

[17] J. Yoon *et al.*, "A clinically translatable hyperspectral endoscopy (HySE) system for imaging the gastrointestinal tract," *Nature Communications*, vol. 10, no. 1, p. 1902, Apr. 2019, doi: 10.1038/s41467-019-09484-4.

[18] A. S. Luthman *et al.*, "Bimodal reflectance and fluorescence multispectral endoscopy based on spectrally resolving detector arrays," *J. Biomed. Opt.*, vol. 24, no. 03, p. 1, Oct. 2018, doi: 10.1117/1.JBO.24.3.031009.

[19] M. Hohmann *et al.*, "*In-vivo* multispectral video endoscopy towards *in-vivo* hyperspectral video endoscopy," *Journal of Biophotonics*, vol. 10, no. 4, pp. 553–564, Apr. 2017, doi: 10.1002/jbio.201600021.

[20] J. Shapey *et al.*, "Intraoperative multispectral and hyperspectral label-free imaging: a systematic review of in vivo clinical studies," *Journal of Biophotonics*, p. e201800455, Mar. 2019, doi: 10.1002/jbio.201800455.